



Biosorption of uranium from aqueous solutions by *Azolla* sp. and *Limnobium laevigatum*

Leandro Goulart de Araujo¹ · Ludmila Cabreira Vieira¹ · Rafael Luan Sehn Canevesi² · Edson Antonio da Silva² · Tamires Watanabe¹ · Rafael Vicente de Padua Ferreira³ · Júlio Takehiro Marumo¹

Received: 22 October 2021 / Accepted: 4 February 2022 / Published online: 10 February 2022
© The Author(s), under exclusive licence to Springer-Verlag GmbH Germany, part of Springer Nature 2022

Abstract

The main goal of this study was to assess alternatives to the current challenges on environmental quality and circular economy. The former is here addressed by the treatment of radioactively contaminated solutions, and the latter by using abundant and low-cost biomass. In this paper, we examine the biosorption of hexavalent uranium (U(VI)) in a batch system using the macrophytes *Limnobium laevigatum* and *Azolla* sp. by three operational parameters: biomass dose, metal ion concentration, and contact time. Simulated solutions were firstly addressed with two biomasses, followed by studies with real liquid organic radioactive waste (LORW) with *Azolla* sp. The batch experiments were carried out by mixing 0.20 g biomass in 10 mL of the prepared solution or LORW. The total contact time employed for the determination of the equilibrium times was 240 min, and the initial U(VI) concentration was 0.63 mmol L⁻¹. The equilibrium times were 15 min for *L. laevigatum* and 30 min for *Azolla* sp. respectively. A wide range of initial U(VI) concentrations (0.25–36 mmol L⁻¹) was then used to assess the adsorption capacity of each macrophyte. Isotherm models validated the adsorption performance of the biosorption process. *Azolla* sp. presented a much higher U(VI) uptake (0.474 mmol g⁻¹) compared to *L. laevigatum* (0.026 mmol g⁻¹). When in contact with LORW, *Azolla* sp. removed much less uranium, indicating an adsorption capacity of 0.010 mmol g⁻¹. In conclusion, both biomasses, especially *Azolla* sp., can be used in the treatment of uranium-contaminated solutions.

Keywords Biosorption · Uranium · Radioactive waste management · *Limnobium laevigatum* · *Azolla* sp

Responsible Editor: Tito Roberto Cadaval Jr.

Highlights

- *Azolla* sp. uptook much more U than *Limnobium laevigatum*.
- Equilibrium was reached in less than 30 min.
- In contact with real radioactive waste, U removal was significantly lower.
- Sips model best represented the biosorption of U(VI) by *Azolla* sp.

✉ Leandro Goulart de Araujo
lgoulart@alumni.usp.br

- ¹ IPEN/CNEN, Av. Prof. Lineu Prestes, Instituto de Pesquisas Energéticas e Nucleares, 2242 – Cidade Universitária, Sao Paulo, SP 05508-000, Brazil
- ² Universidade Estadual do Oeste do Paraná, Rua da Faculdade 645 - Jardim La Salle, Toledo, PR 85903-000, Brazil
- ³ Itatijuca Biotech, Av. Prof. Lineu Prestes, 2242 Cidade Universitária, Sao Paulo, SP 05508-000, Brazil

Introduction

Research related to the use of new materials for the treatment of water, wastewater, and radioactive liquid waste containing organic and inorganic pollutants remains a topic of interest. This is due to concerns raised in recent decades about the dangers of these wastes to human health. Recently, a variety of materials has been used in this context, such as metal–organic framework membranes (Yu et al. 2021), biochar-based composites (Liang et al. 2021; Qiu et al. 2021), yttrium silicate (Litrenta Medeiros et al. 2020), hydroxyapatite, and bone meal (Watanabe et al. 2021), *Saccharomyces cerevisiae*–calcium alginate beads (de Araujo et al. 2020), and SF₆S@Biochar composites (Liu et al. 2021b).

Finding alternatives for radioactive waste management that combine low cost and efficiency is an important and difficult task given to the nature of such waste. Among all the radioactive elements, great attention has been focused on uranium. A large amount of effluent containing uranium is annually produced from numerous nuclear-based activities,

such as uranium exploration and processing, production of nuclear power and nuclear weapons, and disposal of radioactive waste (Yang et al. 2017; Su et al. 2019).

Uranium is highly toxic, radioactive, and it is considered one of the most dangerous heavy metals in the environment. The main concerns about this compound are the possibility of reaching the ecological food chain, harming human being's health. Furthermore, long-term exposure to this radioelement can cause lung cancer, kidney and liver impairment, besides physical-related malformations (Hon et al. 2015). The ecological pollution and toxicity associated with uranium stimulated researchers to investigate efficient and rapid methods for its removal. Among treatment processes, biosorption has attracted attention due to the sludge-free operation, and the use of non-value wastes that are easy to acquire and to handle and may possess a significant regeneration capacity (Bağda et al. 2017; Ecer and Şahan 2018; Yılmaz et al. 2018).

Macrophytes have been utilized for uranium removal (Mkandawire et al. 2004; Charles et al. 2006; Pratas et al. 2012, 2014; Yi et al. 2016b, a, 2018; Vieira et al. 2019). Nevertheless, studies with *Limnobium laevigatum* and *Azolla* sp. are scarce in the literature regarding their use as biosorbents for the removal of metals, and notably uncommon are investigations with radionuclides. *Limnobium laevigatum* (Humb. & Bonpl. Ex Willd) Heine belongs to the family *Hydrocharitaceae* and is a free, perennial floating aquatic macrophyte with short petioles, circular leaves arranged in rosettes with bright free edges (Catian et al. 2012). Although it has previously been used effectively in the phytoextraction of Pb, Cr, Ni, and Zn (Arán et al. 2017; San Juan et al. 2018), and in the removal of N and P (Sudiarto et al. 2019), the potential of *L. laevigatum* is still unclear, especially with dead biomass, i.e., excluding the effects of bioaccumulation.

The water fern, the popular name for *Azolla* sp., is a small floating aquatic macrophyte belonging to the *Azollaceae* family and is in the same class as the avenca and ferns (*Pteridophytes*). (Ghorbanzadeh Mashkani and Tajer Mohammad Ghazvini 2009) employed *Azolla filiculoides* for biosorption of Cs and Sr. In optimum conditions, the authors achieved the maximum uptake capacities of 195 mg g⁻¹ and 212.1 mg g⁻¹ for Cs and Sr ions, respectively. They concluded that given the high adsorption capacity of *Azolla filiculoides* and its abundance worldwide, there is a potential of using this natural floating fern for wastewater treatment in the future.

In this paper, we investigate *L. laevigatum* and *Azolla* sp. as biosorbents of U(VI) in contaminated solutions through three operational parameters: biomass dose, metal ion concentration, and contact time. The two macrophytes are compared in terms of equilibrium time and removal capacity considering their morphological characteristics and predictions using kinetics and isotherm models. Simulated

solutions were firstly addressed with both biomasses, followed by studies with real liquid organic radioactive waste (LORW) with *Azolla* sp. To the best of our knowledge, phytoremediation of U(VI) with these macrophytes has not been already considered, particularly to treat actual radioactive waste. Identifying an effective use for these macrophytes is not only environmentally advantageous but also brings economic rewards due to the use of inexpensive biomass.

Materials and methods

The experimental conditions are briefly given in Fig. 1 (see also Supplementary Information).

In short, raw biomass was sieved and only particle sizes between 0.297 and 0.125 mm were used. For the experiments with synthetic solutions (uranium only), pH was initially fixed at 4, mainly because it is the speciation of U(VI) in water (Yang and Volesky 1999). The components (biomass/solution) were mixed in an orbital shaker (Biothec, Brazil), and the stirring speed and temperature were kept at 130 rpm and 21 °C, respectively. The contact times were 5, 30, 60, 120, and 240 min, selected from exploratory studies. Afterward, we used filtration to isolate the biomass (slow filtration for fine precipitates; ash content of 0.00012 g) (Millipore, USA).

The characterization steps included (i) morphology; (ii) real and apparent densities; (iii) specific surface areas; and (iv) analysis of atomic absorption spectroscopy (AAS) in the infrared region with Fourier transform. The determination of U(VI) and U(total) were performed by inductively coupled plasma optical emission spectroscopy (ICP-OES), model Optima 7000DV (Perkin Elmer, USA).

To check for the applicability of these macrophytes in real contaminated solutions, we also conducted experiments with LORW. The selected waste is from research and development activities from IPEN's IEA-R1 research reactor. LORW is mainly composed of water; ethyl acetate (196 mg L⁻¹); tributyl phosphate (227 mg L⁻¹); [U(total)] (0.25 mmol L⁻¹); and other compounds and radionuclides (Ferreira et al. 2013). The pH value is 3 because of the considerable amount of nitric acid in the liquid waste.

Biosorption experiments

The experiments were performed in a batch system and in triplicate for each macrophyte. Ten milliliters of prepared or liquid waste solution was mixed with the biomass (0.2 g). In Step 1 (Fig. 1), kinetics experiments were carried out by using 0.63 mmol L⁻¹ as the initial U(VI) concentration, and the equilibrium time was determined. Based on the data generated in Step 1, the equilibrium time was fixed, and the initial U(VI) concentration varied from 0.25 to 36 mmol L⁻¹.

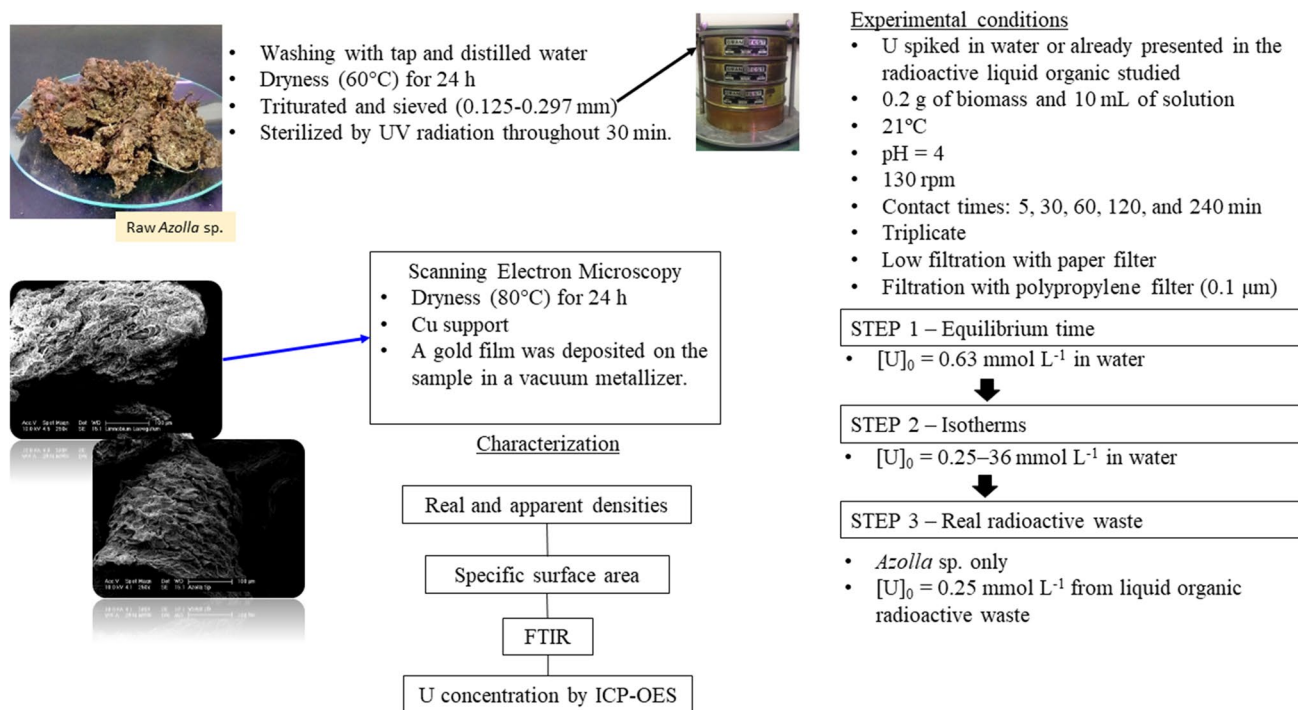


Fig. 1 Simplified diagram of the procedures undertaken in the characterization of biomass and experimental conditions (for more information, see Supplementary Information)

Isotherms were then obtained (Step 2). In Step 3, we evaluated the efficiency of *Azolla* sp. in removing U(total) from LORW. The kinetics and equilibrium were again determined.

Mathematical modeling

Three different isotherm models were applied to describe the adsorption equilibrium isotherms: Langmuir, Freundlich, and Sips. Lagergren's pseudo-first-order and pseudo-second-order models were selected for the kinetics analyzes of uranium biosorption by *Azolla* sp. and *L. laevigatum*. The Akaike Information Criterion (AIC) was used to check the isotherm models (see Supplementary Information for the complete description of the isotherms and equations of the mathematical modeling used).

Results and discussion

Characterization

Both biomasses were analyzed by scanning electron microscopy and energy dispersive X-ray spectrometry (SEM–EDS) to verify their morphological characteristics and chemical compositions, respectively. Figure 2 illustrates the micrographs and EDS spectra for *L. laevigatum* and *Azolla* sp.

Figure 2 highlights that *L. laevigatum* and *Azolla* sp. possess irregular structures and have a similar appearance. Despite the distinct aspect of their surfaces, their morphologies are very characteristic of macrophytes (Pelosi et al. 2014; Lima et al. 2015; Vieira et al. 2019). Both depicted a rough surface and the presence of microstructures, which according to Lima et al. (2015) can be ascribed to the deposition of salts on the surface of the macrophytes. *Azolla* sp. revealed a high percentage of Si whereas *L. laevigatum* has a high percentage of Ca. Both presented a significant presence of K (see Supplementary Information for the complete EDS data, Table S1).

L. laevigatum (densities: (real) $1.550 \pm 0.001 \text{ g cm}^3$ and (apparent) $0.320 \pm 0.010 \text{ g cm}^3$) and *Azolla* sp. (density: (real) $1.500 \pm 0.003 \text{ g cm}^3$ and (apparent) $0.250 \pm 0.020 \text{ g cm}^3$) highlighted similar values in terms of density and, accordingly to the SEM analysis, their aspect is analogous. The specific surface area was measured and *Azolla* sp. pinpointed a much larger specific surface area (*Azolla* sp.: $14.00 \pm 1.00 \text{ m}^2 \text{ g}^{-1}$ versus *Limnobium laevigatum*: $3.10 \pm 0.30 \text{ m}^2 \text{ g}^{-1}$). Having *Azolla* sp. a significantly higher surface area, higher adsorption capacity is expected, considering that both present similar features regarding morphology, element composition, and density. *L. laevigatum* and *Azolla* sp. functional groups are displayed by mid-infrared (mid-IR) (Fig. 3).

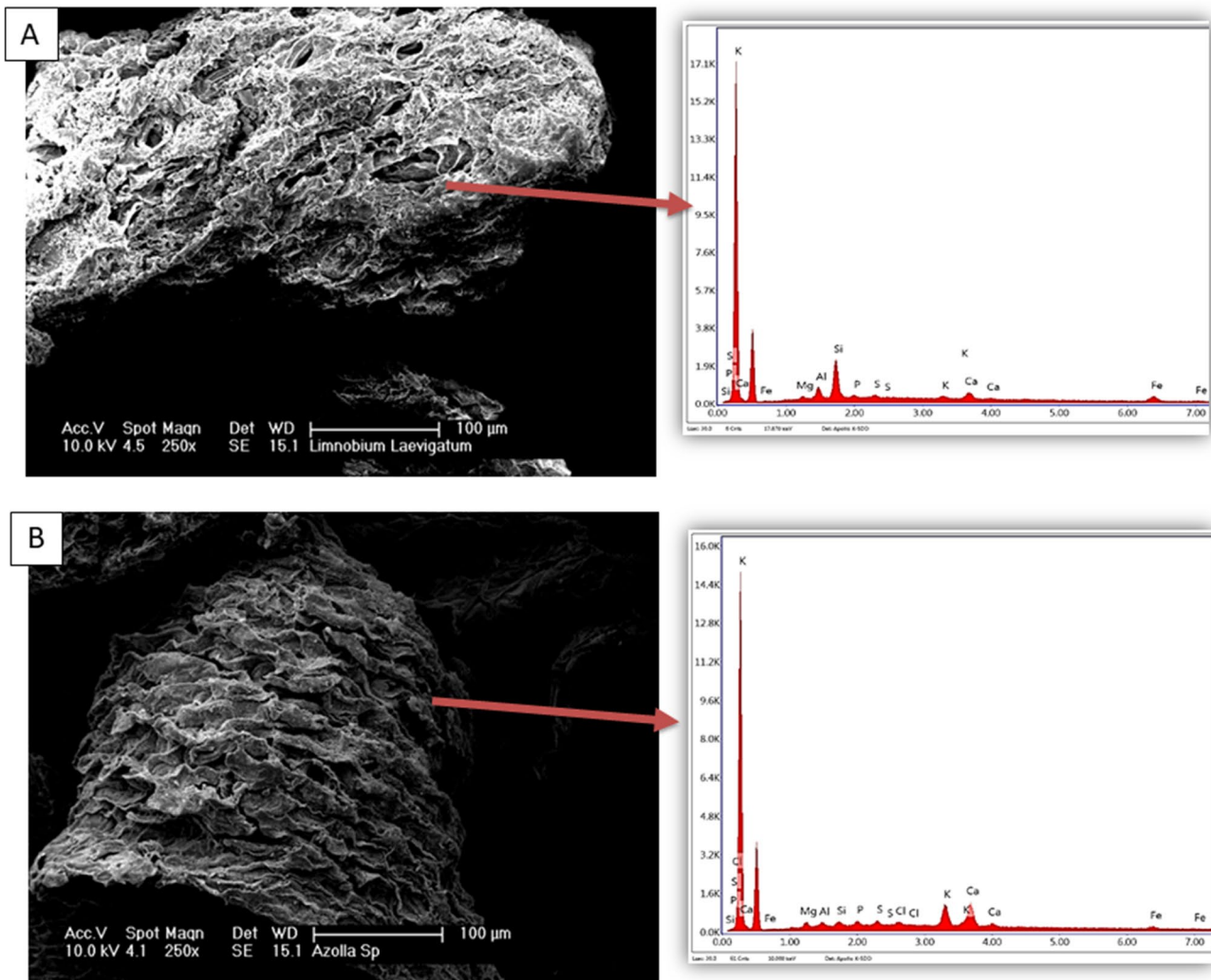


Fig. 2 Micrograph and EDS spectra of each biomass **A** *Limnobium laevigatum* (raw form); **B** *Azolla* sp. (raw form)

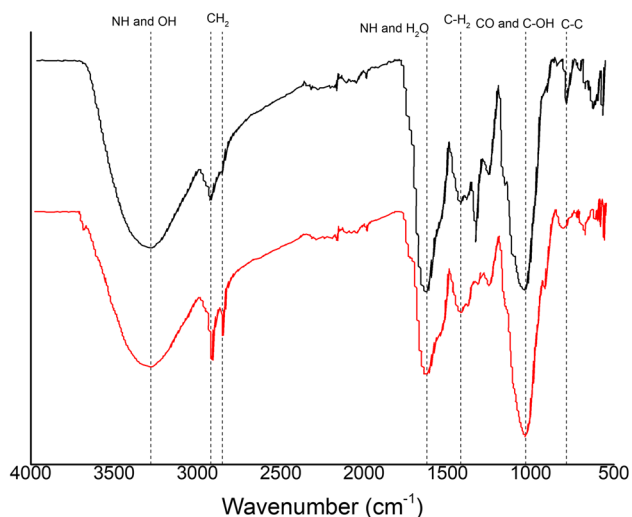


Fig. 3 Mid-infrared spectra of (black line) *Limnobium laevigatum* and (red line) *Azolla* sp

The bands located at 3280 cm^{-1} for *L. laevigatum* and 3279 cm^{-1} for *Azolla* sp. highlight an overlap of NH and OH (Tuzen et al. 2008; Vieira et al. 2019). The band 2920 cm^{-1} of the *L. laevigatum* spectrum and the 2917 cm^{-1} and 2850 cm^{-1} bands in the *Azolla* sp. spectrum are assigned to the asymmetric and symmetric vibration of methylene (CH_2) (Lima et al. 2016). The bands located at 1618 cm^{-1} and 1624 cm^{-1} represent the amine group (NH) and water (Salman et al. 2010; Drumm et al. 2020; Rigueto et al. 2020). The band located at 1420 cm^{-1} is the C-H_2 stretching bending (Ardila et al. 2017). The stretching vibrations of CO with single bonds and C–OH are present in the 1030 cm^{-1} band for both *L. laevigatum* and *Azolla* sp. (Sari and Tuzen 2009; Drumm et al. 2020). Finally, the band located at 806 cm^{-1} is due to $-\text{C}-\text{C}$ (Ferreira et al. 2020).

The mid-IR of *Azolla* sp. is especially similar to the mid-IR of *Lemma* sp., whereas the mid-IR of *L. laevigatum* resembles that of the *Pistia stratiotes* (Vieira et al. 2019).

Fig. 4 Experimental data and model kinetics for U(VI) adsorption by the macrophytes. (filled square) experimental data; (dashed line) pseudo-first-order model; (dot line) pseudo-second-order model. **A** *Limnobium laevigatum* and **B** *Azolla* sp. $[U(VI)]_0 = 0.63 \text{ mmol L}^{-1}$

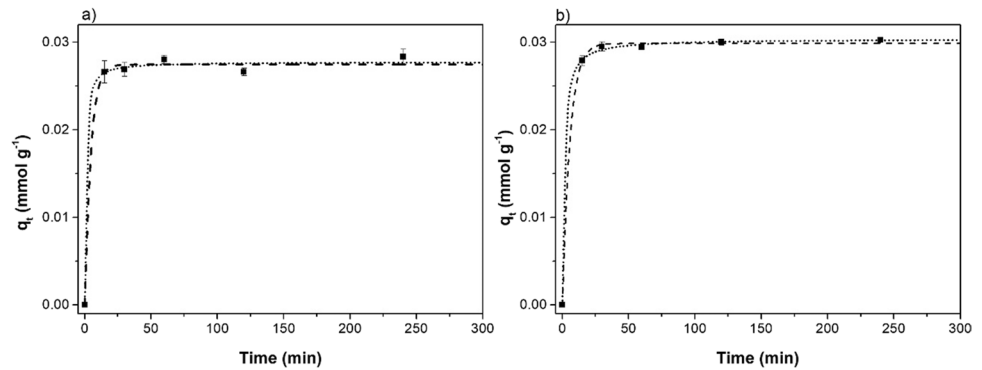


Table 1 Parameters of the calculated kinetics for each biomass

| Model | Macrophyte | | |
|---------------------|---|-----------------------------|-------------------|
| | | <i>Limnobium laevigatum</i> | <i>Azolla</i> sp. |
| Pseudo-first-order | q_{eq} (mmol g ⁻¹) | 0.027 | 0.030 |
| | K_1 (min ⁻¹) | 0.275 | 0.180 |
| | R^2 | 0.997 | 0.999 |
| Pseudo-second-order | q_{eq} (mmol g ⁻¹) | 0.028 | 0.030 |
| | K_2 (g mmol ⁻¹ min ⁻¹) | 51.7 | 26.0 |
| | R^2 | 0.998 | 1.000 |

According to Yi et al. (2016a, b), the amine and carboxyl groups are the main groups that provide uranium biosorption by the macrophyte *Eichhornia crassipes*.

Biosorption assays

Biosorption kinetics

The first biosorption assays aimed at reaching the equilibrium time with the initial U(VI) concentration of 0.63 mmol L^{-1} and a total contact time of 240 min. Figure 4 depicts the adsorption capacity of each macrophyte as a function of time.

As expected, the adsorption of uranium by both macrophytes increased over time until equilibrium was reached. In terms of uranium removal capacity in equilibrium (q_e) in this specific experimental condition that the kinetic experiment was carried out, the values were similar for the two adsorbents ($q_e, L. laevigatum = 0.028 \text{ mmol g}^{-1}$; $q_e, Azolla \text{ sp.} = 0.030 \text{ mmol g}^{-1}$). The equilibrium time was reached after 15 min for *L. laevigatum* and 30 min for *Azolla* sp. This can also be confirmed by the values of the parameters of the kinetic constants K_1 and K_2 (Table 1), which were all superior to *L. laevigatum* than to *Azolla* sp. The higher the values of these parameters, the steeper the curve and the faster the equilibrium time is reached. Despite reaching

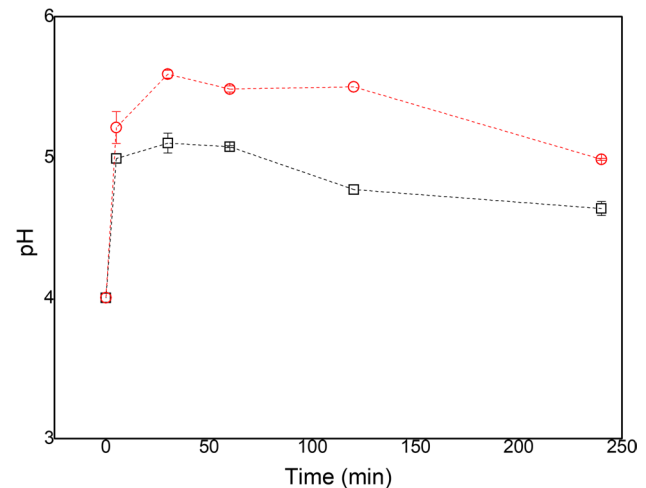


Fig. 5 pH variation for (red circle) *Azolla* sp. in contact with the synthetic solution; (black square) *Limnobium laevigatum* in contact with the synthetic solution

equilibrium faster, *Azolla* sp. indicated slightly superior values of adsorption capacity, which may have increased the time for reaching equilibrium. Both pseudo-first-order and pseudo-second-order were used to predict adsorption by using the experimental data. The parameters obtained in the kinetic models are listed in Table 1.

Both pseudo-models indicated high correlation coefficient (R^2) values (> 0.997). However, the pseudo-second order model best represented uranium biosorption by both macrophytes. This corroborates with the mechanism of U removal by other authors with the use of persimmon tannin functionalized waste paper (Liu et al. 2022) and $\text{Fe}_3\text{O}_4@ \text{MnOx}$ with 3D hollow structure (Zhang et al. 2021), who found R^2 values of 0.975 and 0.992 for the pseudo-second order model, respectively.

Initial pH was initially fixed at 4 and its changes over time were assessed. Figure 5 shows the temporal evolution of the pH during these adsorption experiments.

After 5 min of mixing, the pH values changed from 4 to about 5. The maximum pH was 5.59 ± 0.03 , reached at

30 min. Cordeiro et al. (2016) found that U tends to accumulate in plant roots due to U complexation with phosphate. According to Xiong et al. (2021), there are three mechanisms that may occur in the removal of U(IV) by materials that have phosphate and calcium in their composition: adsorption, dissolution–precipitation, and ion-exchange. The observed increase in pH suggests that dissolution–precipitation was likely the major process during our experiments. The acidic conditions of the solutions may have released Ca^{2+} and PO_4^{3-} that reacted with U(VI), forming compounds such as $\text{Ca}(\text{UO}_2)_2(\text{PO}_4)_2 \cdot 3\text{H}_2\text{O}$ (Watanabe et al. 2021). A slight decrease in pH was then observed over time, probably given to the sorption of the hydroxide forms of uranium in the macrophytes. The narrow variations noticed in the tests provide a good indication that the adsorption process was stable.

Biosorption capacity

In Step 2, the time taken to reach equilibrium was fixed for the isotherm study. Initial uranium concentrations varied from 0.25 to 36 mmol L^{-1} . The values of the parameters calculated by the isotherms and the statistical parameters R^2 and AIC for both macrophytes are listed in Table 2, followed

by the experimental versus predicted data from the isotherm models (Fig. 6).

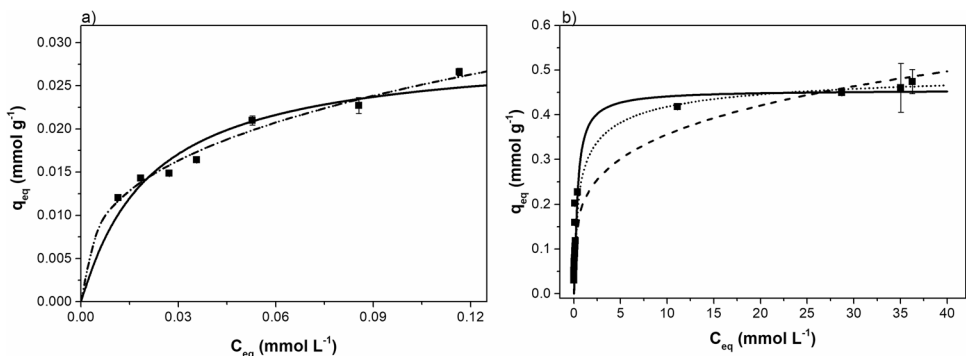
Azolla sp. presented a much higher sorption ability with $0.47 \pm 0.05 \text{ mmol g}^{-1}$ compared to that of the *L. laevigatum*, $0.027 \pm 0.0009 \text{ mmol g}^{-1}$ (Fig. 6). The much larger specific relative area of the *Azolla* sp. ($14.00 \pm 1.00 \text{ m}^2 \text{ g}^{-1}$) compared to *L. laevigatum* ($3.10 \pm 0.30 \text{ m}^2 \text{ g}^{-1}$) may have contributed to the improved U(VI) uptake, given the expected higher availability of the adsorption sites. Vieira et al. (2019) presented similar results for *Lemna* sp. and *Pistia stratiotes* with 0.68 mmol g^{-1} and $0.029 \text{ mmol g}^{-1}$, respectively, both after 1 h. However, *Lemna* sp. and *P. stratiotes* indicated an equilibrium time of 1 h, as opposed to *L. laevigatum* and *Azolla* sp. which were 15 and 30 min, respectively. For *L. laevigatum*, the Freundlich and Sips models presented the best fit. The exponent β (0.34) indicates a trend for both Sips and Freundlich. The Freundlich constant ($1/n$) indicates that adsorption occurred favorably (Zhang et al. 2021). For *Azolla* sp., Sips better represented the experimental data ($R^2=0.97$, $\text{AIC} = -113$).

The maximum absorption capacities of U(VI) on *L. laevigatum* and *Azolla* sp. calculated from the Langmuir model were 0.03 and 0.46 mmol g^{-1} , respectively. *Azolla* sp. capacity is significantly higher than other biosorbents such as active yeast cells entrapped in gel beads (0.14 mmol g^{-1})

Table 2 Parameters calculated from the selected adsorption models for each biomass and the correlation coefficients obtained for each model

| Biomass | Model | R^2 | AIC | Parameters | | |
|-----------------------------|------------|-------|------|--------------------------------|--------------------------------|-----------|
| <i>Limnobium laevigatum</i> | Langmuir | 0.91 | -85 | Q (mmol g^{-1}) | K_L (L mmol^{-1}) | |
| | | | | 0.03 | 0.46 | |
| | Freundlich | 0.97 | -94 | K_f (L mmol^{-1}) | $1/n$ | |
| | | | | 5.4×10^{-2} | 0.35 | |
| | Sips | 0.97 | -92 | K_s (L mmol^{-1}) | a_s (L mmol^{-1}) | β_s |
| | | | | 5.5×10^{-2} | 8.9×10^{-4} | 0.34 |
| <i>Azolla</i> sp. | Langmuir | 0.96 | -111 | Q (mmol g^{-1}) | K_L (L mmol^{-1}) | |
| | | | | 0.46 | 3.0 | |
| | Freundlich | 0.95 | -107 | K_f (L mmol^{-1}) | $1/n$ | |
| | | | | 4.1 | 0.24 | |
| | Sips | 0.97 | -113 | K_s (L mmol^{-1}) | a_s (L mmol^{-1}) | β_s |
| | | | | 0.58 | 1.1 | 0.59 |

Fig. 6 Experimental versus predicted values for the biosorption of U(VI) using the macrophytes **A** *Limnobium laevigatum* and **B** *Azolla* sp. (black square) experimental data, (—) Langmuir isotherm model, (•••) Freundlich Isotherm model, and (---) Sips Isotherm models



(Chen et al. 2020), *Candida utilis* (0.17 mmol g⁻¹) (Liu et al. 2021a), and *Pistia stratiotes* (0.04 mmol g⁻¹) (Vieira et al. 2019). On the other hand, higher capacities were also found, for instance those obtained for *Hydrilla verticillate* (0.72 mmol g⁻¹) (Yi et al. 2017), and *Lemna* sp. (0.74 mmol g⁻¹) (Vieira et al. 2019). Note that these values are highly dependent on U(VI) concentration, pH, and adsorbent mass. In general terms, the values obtained in this work are comparable to other natural-based adsorbents.

There are few reports on the biosorption of U(VI) by macrophytes. Nevertheless, there are data on the biosorption of other metals. For instance, Yi et al. (2016a, b) employed *Eichhornia crassipes* for biosorption of U(VI) in synthetic uranium-contaminated solutions, obtaining an adsorption capacity closer to ours (0.6 mmol g⁻¹). Charles et al. (2006) employed *Lemna aequinoctialis* in individually or mixed contaminated solutions by U and/or Cu. The authors highlight that the toxicity of both metals affects the growth of this macrophyte as a result of bioaccumulation. Pratas et al. (2014) used three macrophytes for uranium bioaccumulation. These macrophytes were *Callitriche stagnalis* Scop, *Potamogeton natans* L., and *Potamogeton pectinatus* L. The latter indicated the best results, with 6.55×10^{-3} mmol g⁻¹.

Finally, in Step 3, *Azolla* sp. was used in biosorption kinetic tests with the LORW in a batch reactor. The reason is that *Azolla* sp. highlighted a much higher U(VI) uptake in the aqueous solutions (water and uranium nitrate) when compared to *L. laevigatum*.

Azolla sp. presented a sorption capacity of $10.92 \times 10^{-3} \pm 1.26 \times 10^{-3}$ mmol g⁻¹ when in contact with the LORW. This value is slightly superior to that obtained for *Lemna* sp. (9.24×10^{-3} mmol g⁻¹) (Vieira et al. 2019) and coffee and rice husks with 8.24×10^{-3} mmol g⁻¹ and 3.35×10^{-3} mmol g⁻¹, respectively (Ferreira et al. 2020). Furthermore, *Azolla* sp. sorption capacity is also higher than that of coconut fiber, which was 7.65×10^{-3} mmol g⁻¹ (Ferreira et al. 2018).

Synthetic solutions presented much higher sorption values for uranium than the actual radioactive waste, which is expected given to the nature of the waste, multi-elementary composition (U, Pu, Am, Cs, and others), and the presence of organic compounds (ethyl acetate and tributyl phosphate). No significant changes of pH were observed in function of time.

Conclusions

The effect of two macrophytes, *Limnobia laevigatum*, and *Azolla* sp. on the adsorption of U (VI) in aqueous solutions is presented. *Azolla* sp. presented a much higher sorption ability (0.68 mmol g⁻¹) compared to that of *L. laevigatum*

(0.028 mmol g⁻¹). The greater specific relative area of *Azolla* sp. may have enhanced uranium biosorption. On the other hand, *L. laevigatum* reached equilibrium faster (15 min) than *Azolla* sp. (30 min). The Freundlich and Sips models presented the best fit for *L. laevigatum* as indicated by the exponent β (0.34). In the case of *Azolla* sp., a greater tendency to the model with the Sips ($R^2=0.97$, $AIC=-113$) denotes a less heterogeneous surface for this material. The last can also be identified by the values of the Sips parameter β_s (0.59). The maximum predicted absorption capacities of U(VI) on *Azolla* sp. and *L. laevigatum* were 0.46 and 0.03 mmol g⁻¹, respectively. pH increase during the beginning of the experiments is an indication that dissolution–precipitation was likely the main process because of the presence of calcium and phosphate in both macrophytes, followed by a slight decrease in pH due to the sorption of the hydroxide forms of uranium. Furthermore, the limited pH variations indicated that the adsorption process was steady. *Azolla* sp. sorption capacity, when applied to a real radioactive waste, was significantly inferior (0.01 mmol g⁻¹). The reasons are due to the complex nature of the radioactive liquid, which may have hindered uranium removal. The macrophytes were considered as an easy approach to be used as biosorbents for uranium-contaminated water sources.

Supplementary Information The online version contains supplementary material available at <https://doi.org/10.1007/s11356-022-19128-8>.

Acknowledgements This study was supported by the Nuclear and Energy Research Institute, the National Nuclear Energy Commission, and the National Council of Technological and Scientific Development.

Author contribution Leandro Goulart de Araujo: conceptualization, formal analysis, investigation, methodology, writing — original draft; Ludmila Cabrera Vieira: data curation, investigation, resources, visualization; Tamires Watanabe: data curation, investigation; Rafael Luan Sehn Canevesi: data curation, investigation, writing — review and editing; Edson Antônio da Silva: resources, visualization, supervision, writing — review and editing; Rafael Vicente de Padua Ferreira: data curation, supervision; Júlio Takehiro Marumo: conceptualization, formal analysis, methodology, project administration, resources, visualization, writing —review and editing. All the authors read and approved the final manuscript.

Data availability All the data generated or analyzed during this study are included in this published article and its supplementary information.

Declarations

Ethics approval Not applicable.

Consent to participate Not applicable.

Consent for publication Not applicable.

Competing interests The authors declare no competing interests.

References

- Arán DS, Harguinteguy CA, Fernandez-Cirelli A, Pignata ML (2017) Phytoextraction of Pb, Cr, Ni, and Zn using the aquatic plant *Limnobiium laevigatum* and its potential use in the treatment of wastewater. *Environ Sci Pollut Res* 24:18295–18308
- Ardila N, Daigle F, Heuzey M-C, Aji A (2017) Antibacterial activity of neat chitosan powder and flakes. *Molecules* 22:100. <https://doi.org/10.3390/molecules22010100>
- Bağda E, Tuzen M, Sarı A (2017) Equilibrium, thermodynamic and kinetic investigations for biosorption of uranium with green algae (*Cladophora hutchinsiae*). *J Environ Radioact* 175–176:7–14. <https://doi.org/10.1016/j.jenvrad.2017.04.004>
- Catian G, Leme FM, Francener A et al (2012) Macrophyte structure in lotic-lentic habitats from Brazilian Pantanal. *Oecologia Aust* 16:782–796. <https://doi.org/10.4257/oeco.2012.1604.05>
- Charles AL, Markich SJ, Ralph P (2006) Toxicity of uranium and copper individually, and in combination, to a tropical freshwater macrophyte (*Lemna aquinoctialis*). *Chemosphere* 62:1224–1233. <https://doi.org/10.1016/J.CHEMOSPHERE.2005.04.089>
- Chen C, Hu J, Wang J (2020) Uranium biosorption by immobilized active yeast cells entrapped in calcium-alginate-PVA-GO-crosslinked gel beads. *Radiochim Acta* 108:273–286. <https://doi.org/10.1515/ract-2019-3150>
- Cordeiro C, Favas PJ, Pratas J et al (2016) Uranium accumulation in aquatic macrophytes in an uraniumiferous region: relevance to natural attenuation. *Chemosphere* 156:76–87. <https://doi.org/10.1016/j.chemosphere.2016.04.105>
- de Araujo LG, De Borba TR, de Pádua Ferreira RV et al (2020) Use of calcium alginate beads and *Saccharomyces cerevisiae* for biosorption of ²⁴¹Am. *J Environ Radioact* 223:106399. <https://doi.org/10.1016/j.jenvrad.2020.106399>
- Drumm FC, Franco DSP, Georgin J, et al (2020) Macro-fungal (*Agaricus bisporus*) wastes as an adsorbent in the removal of the acid red 97 and crystal violet dyes from ideal colored effluents. *Environ Sci Pollut Res* 28:405–415. <https://doi.org/10.1007/s11356-020-10521-9>
- Ecer Ü, Şahan T (2018) A response surface approach for optimization of Pb (II) biosorption conditions from aqueous environment with *Polyporus squamosus* fungi as a new biosorbent and kinetic, equilibrium and thermodynamic studies. *Desalin Water Treat* 102:229–240. <https://doi.org/10.5004/dwt.2018.21871>
- Ferreira RVP, Silva EA, Canevesi RLS et al (2018) Application of the coconut fiber in radioactive liquid waste treatment. *Int J Environ Sci Technol* 15:1629–1640. <https://doi.org/10.1007/s13762-017-1541-6>
- Ferreira EGA, Ferreira RVP, Araujo LG, et al (2013) Chemical analysis of radioactive mixed liquid wastes by alpha/gamma spectrometry, ICP-OES and Arsenazo III. International Nuclear Atlantic Conference, Recife, PE, Brazil.
- Ferreira RV de P, de Araujo LG, Canevesi RLS, et al (2020) The use of rice and coffee husks for biosorption of U (total), ²⁴¹Am, and ¹³⁷Cs in radioactive liquid organic waste. *Environ Sci Pollut Res* 27:36651–36663. <https://doi.org/10.1007/s11356-020-09727-8>
- Ghorbanzadeh Mashkani S, Tajer Mohammad Ghazvini P (2009) Biotechnological potential of *Azolla filiculoides* for biosorption of Cs and Sr: application of micro-PIXE for measurement of biosorption. *Bioresour Technol* 100:1915–1921. <https://doi.org/10.1016/j.biortech.2008.10.019>
- Hon Z, Österreicher J, Navrátil L (2015) Depleted uranium and its effects on humans. *Sustain* 7:4063–4077. <https://doi.org/10.3390/su7044063>
- Liang L, Xi F, Tan W et al (2021) Review of organic and inorganic pollutants removal by biochar and biochar-based composites. *Biochar* 3:255–281. <https://doi.org/10.1007/s42773-021-00101-6>
- Lima L, Bento C, Silva M, Vieira M (2015) Fixed bed biosorption using aquatic macrophyte in lead removal. *Blucher Chem Eng Proc* 1:6425–6432. <https://doi.org/10.5151/chemeng-cobeq-2014-1996-16493-145673>
- Lima LKS, Silva MGC, Vieira MGA (2016) Study of binary and single biosorption by the floating aquatic macrophyte *Salvinia natans*. *Brazilian J Chem Eng* 33:649–660. <https://doi.org/10.1590/0104-6632.20160333s20150483>
- Litrenta Medeiros V, de Araujo LG, Rubinho Ratero D et al (2020) Synthesis and physicochemical characterization of a novel adsorbent based on yttrium silicate: a potential material for removal of lead and cadmium from aqueous media. *J Environ Chem Eng* 8:103922. <https://doi.org/10.1016/j.jece.2020.103922>
- Liu L, Chen J, Liu F et al (2021a) Bioaccumulation of uranium by *Candida utilis*: investigated by water chemistry and biological effects. *Environ Res* 194:110691. <https://doi.org/10.1016/j.envres.2020.110691>
- Liu F, Hua S, Wang C, Hu B (2022) Insight into the performance and mechanism of persimmon tannin functionalized waste paper for U (VI) and Cr (VI) removal. *Chemosphere* 287:132199. <https://doi.org/10.1016/j.chemosphere.2021.132199>
- Liu R, Wang H, Han L, et al (2021b) Reductive and adsorptive elimination of U (VI) ions in aqueous solution by SFeS@ Biochar composites. *Environ Sci Pollut Res* 28:55176–55185. <https://doi.org/10.1007/s11356-021-14835-0>
- Mkandawire M, Taubert B, Dudel EG (2004) Capacity of *Lemna gibba* L. (duckweed) for uranium and arsenic phytoremediation in mine tailing waters. *Int J Phytoremediation* 6:347–362. <https://doi.org/10.1080/16226510490888884>
- Pelosi BT, Lima LKS, Vieira MGA (2014) Removal of the synthetic dye Remazol Brilliant Blue R from textile industry wastewaters by biosorption on the macrophyte *Salvinia natans*. *Brazilian J Chem Eng* 31:1035–1045. <https://doi.org/10.1590/0104-6632.20140314s00002568>
- Pratas J, Favas PJC, Paulo C et al (2012) Uranium accumulation by aquatic plants from uranium-contaminated water in Central Portugal. *Int J Phytoremediation* 14:221–234. <https://doi.org/10.1080/15226514.2011.587849>
- Pratas J, Paulo C, Favas PJC, Venkatachalam P (2014) Potential of aquatic plants for phytofiltration of uranium-contaminated waters in laboratory conditions. *Ecol Eng* 69:170–176. <https://doi.org/10.1016/J.ECOLENG.2014.03.046>
- Qiu M, Hu B, Chen Z, Yang H, Zhuang L, Wang X (2021) Challenges of organic pollutant photocatalysis by biochar-based catalysts. *Biochar* 3:117–123. <https://doi.org/10.1007/s42773-021-00098-y>
- Rigueto CVT, Piccin JS, Dettmer A et al (2020) Water hyacinth (*Eichhornia crassipes*) roots, an amazon natural waste, as an alternative biosorbent to uptake a reactive textile dye from aqueous solutions. *Ecol Eng* 150:105817. <https://doi.org/10.1016/j.ecoleng.2020.105817>
- Salman A, Tsror L, Pomerantz A et al (2010) FTIR spectroscopy for detection and identification of fungal phytopathogens. *Spectroscopy* 24:261–267. <https://doi.org/10.3233/SPE-2010-0448>
- San Juan MRF, Albornoz CB, Larsen K, Najle R (2018) Bioaccumulation of heavy metals in *Limnobiium laevigatum* and *Ludwigia peploides*: their phytoremediation potential in water contaminated with heavy metals. *Environ Earth Sci* 77:1–8. <https://doi.org/10.1007/s12665-018-7566-4>
- Sarı A, Tuzen M (2009) Removal of mercury(II) from aqueous solution using moss (*Drepanocladus revolvens*) biomass: equilibrium, thermodynamic and kinetic studies. *J Hazard Mater* 171:500–507. <https://doi.org/10.1016/j.jhazmat.2009.06.023>
- Su M, Tsang DCW, Ren X et al (2019) Removal of U (VI) from nuclear mining effluent by porous hydroxyapatite: evaluation on characteristics, mechanisms and performance. *Environ Pollut* 254:112891
- Sudiarto SIA, Renggaman A, Choi HL (2019) Floating aquatic plants for total nitrogen and phosphorus removal from treated swine

- wastewater and their biomass characteristics. *J Environ Manage* 231:763–769
- Tuzen M, Dogan M, Uluozlu OD et al (2008) Characterization of biosorption process of As(III) on green algae *Ulothrix cylindricum*. *J Hazard Mater* 165:566–572. <https://doi.org/10.1016/j.jhazmat.2008.10.020>
- Vieira LC, de Araujo LG, de Padua Ferreira RV et al (2019) Uranium biosorption by *Lemna* sp. and *Pistia stratiotes*. *J Environ Radioact* 203:179–186. <https://doi.org/10.1016/j.jenvrad.2019.03.019>
- Watanabe T, Guillen SN, Marumo JT, et al (2021) Uranium biosorption by hydroxyapatite and bone meal: evaluation of process variables through experimental design. *Environ Sci Pollut Res*. <https://doi.org/10.1007/s11356-021-17551-x>
- Xiong T, Li Q, Liao J, et al (2021) Highly enhanced adsorption performance to uranium (VI) by facile synthesized hydroxyapatite aerogel. *J Hazard Mater* 423:127184 <https://doi.org/10.1016/j.jhazmat.2021.127184>
- Yang J, Volesky B (1999) Biosorption of uranium on *Sargassum* biomass. *Water Res* 33:3357–3363. [https://doi.org/10.1016/S0043-1354\(99\)00043-3](https://doi.org/10.1016/S0043-1354(99)00043-3)
- Yang S, Qian J, Kuang L, Hua D (2017) Ion-imprinted mesoporous silica for selective removal of uranium from highly acidic and radioactive effluent. *ACS Appl Mater Interfaces* 9:29337–29344. <https://doi.org/10.1021/acsami.7b09419>
- Yi Z, Yao J, Chen H et al (2016a) Uranium biosorption from aqueous solution onto *Eichhornia crassipes*. *J Environ Radioact* 154:43–51. <https://doi.org/10.1016/J.JENVRAD.2016.01.012>
- Yi Z, Yao J, Kuang Y et al (2016b) Uptake of hexavalent uranium from aqueous solutions using coconut husk activated carbon. *Desalin Water Treat* 3994:1–7. <https://doi.org/10.1080/19443994.2014.977956>
- Yi ZJ, Yao J, Zhu MJ et al (2017) Uranium biosorption from aqueous solution by the submerged aquatic plant *Hydrilla verticillata*. *Water Sci Technol* 75:1332–1341. <https://doi.org/10.2166/wst.2016.592>
- Yi Z, Yao J, Zhu M et al (2018) Biosorptive removal of uranium(VI) from aqueous solution by *Myriophyllum spicatum*. *Desalin Water Treat* 105:273–281. <https://doi.org/10.5004/dwt.2018.22020>
- Yılmaz Ş, Ecer Ü, Şahan T (2018) Modelling and optimization of As (III) adsorption onto thiol-functionalized bentonite from aqueous solutions using response surface methodology approach. *ChemistrySelect* 3:9326–9335. <https://doi.org/10.1002/slct.201801037>
- Yu S, Pang H, Huang S et al (2021) Recent advances in metal-organic framework membranes for water treatment: a review. *Sci Total Environ* 800:149662. <https://doi.org/10.1016/j.scitotenv.2021.149662>
- Zhang T, Chen J, Xiong H, et al (2021) Constructing new Fe₃O₄@MnOx with 3D hollow structure for efficient recovery of uranium from simulated seawater. *Chemosphere* 283:131241 <https://doi.org/10.1016/j.chemosphere.2021.131241>

Publisher's Note Springer Nature remains neutral with regard to jurisdictional claims in published maps and institutional affiliations.